ISSN 0884-5913, Kinematics and Physics of Celestial Bodies, 2012, Vol. 28, No. 2, pp. 69–76. © Allerton Press, Inc., 2012.

EXTRAGALACTIC ASTRONOMY

The Mass Distribution in the Galaxy Cluster Abell 2744[1]

Iu. Babyk[a], A. Elyiv[b, c], O. Melnyk[c, d], and V. N. Krivodubskij[d]

[a] *Faculty of Physics of the Taras Shevchenko National University of Kyiv, Glushkova ave. 4, 03127, Kyiv*
[b] *Main Astronomical Observatory of NAS of Ukraine, Akademika Zabolotnoho str. 27, 03680, Kyiv*
[c] *Institut d'Astrophysique et de Geophysique, Liege, Belgium*
[d] *Astronomical Observatory of the Taras Shevchenko National University of Kyiv, Observatorna str. 3, 04053, Kyiv*
e-mail: babikyura@ukr.net

Received March 13, 2011

Abstract—The mass distribution for the galaxy cluster Abell 2744 ($z = 0.308$) is investigated on the base of the archival X-ray data of the Chandra observatory. The temperature of the hot gas in the cluster ($kT = 9.82^{+0.43}_{-0.41}$ keV) and the cluster total mass ($M_{200} = 2.22^{+0.13}_{-0.12} \times 10^{15}\ M_\odot$) for the radius $R_{200} = 2.38^{+0.36}_{-0.31}$ Mpc are estimated. The density and mass profiles for the intergalactic gas and dark matter are obtained. The fractions of the intergalactic gas and dark matter in the total mass of the cluster are $15.4^{+1.3}_{-1.3}$ % and $84.6^{+1.4}_{-1.3}$ %, respectively.

Keywords: cluster of galaxies, intracluster gas, profile Navarro-Frank-White, dark matter.
DOI: 10.3103/S0884591312020031

1. INTRODUCTION

Galaxy clusters are the largest gravitationally bound structures of our Universe. Clusters have the diameters from 2 to 10 Mpc and total mass within ~ 10^{13}–$10^{15}\ M_\odot$. Since the clusters began to form quite a long time ago (~7–8 billion years ago), they are rightly considered as the unique laboratories in which galaxies are emerged and evolved [16, 26]. Clusters of galaxies consist of gas and dark matter, where the some part of gas, approximately 1% from total mass of cluster, condensates in the form of stars and another, about 10–15% of the total mass of the cluster is an intracluster gas, which is emitted in X-ray [4, 9, 27].

Dark matter is the least studied component of the clusters. The first evidence of dark matter existence had been obtained by Zwicky in 1937 [29] when he was trying to determine the mass of the Coma cluster using the dispersion velocities of galaxies. The distribution of dark matter in clusters has not been clearly understood yet because it is not observed directly. Usually the distribution of dark matter is studied under the assumption that the distribution of hot gas is indirectly related to the distribution of dark matter by means of the hydrostatic equilibrium condition. There are many theoretical models using for a study of the dark matter distribution in the clusters. One of the best models is the density distribution of dark matter by Navarro, Frenk and White (NFW) [19, 20]. The model profile for dark matter of this model is in a good agreement with the observational data [8, 28]. In the work [22], for the reconstruction of the mass profiles in clusters, the authors used model of isothermal sphere, the Moore profile [18] and NFW. On the base of the large sample of galaxy clusters it was shown that the NFW profile reproduces the observations in the best way. Good agreement of the NFW theoretical profile with an experimental data was confirmed also in the other studies by these authors [23, 21].

Intracluster gas is the next component by contamination in the total mass of the cluster. Gas fraction consists of 10–15% of the total mass. Mainly it is the ionized, hydrogen-helium plasma that is enriched with heavy elements with a temperature of several keV. Having such a high temperature, intergalactic gas emits in X-ray range. The spectrum of the radiation has a thermal nature. For the approximation of the density profiles of gas in clusters, so-called β-model [10] is widely used: $\rho_g(r) \sim (1 + r^2/r_c^2)^{-3\beta/2}$, where r_c is the typical cluster core radius, and β is the X-ray brightness profile slope of the cluster (the default values are within 0.6–0.9). For example β-model was used for finding the M–T dependence for a sample of clus-

[1] The article is published in the original.

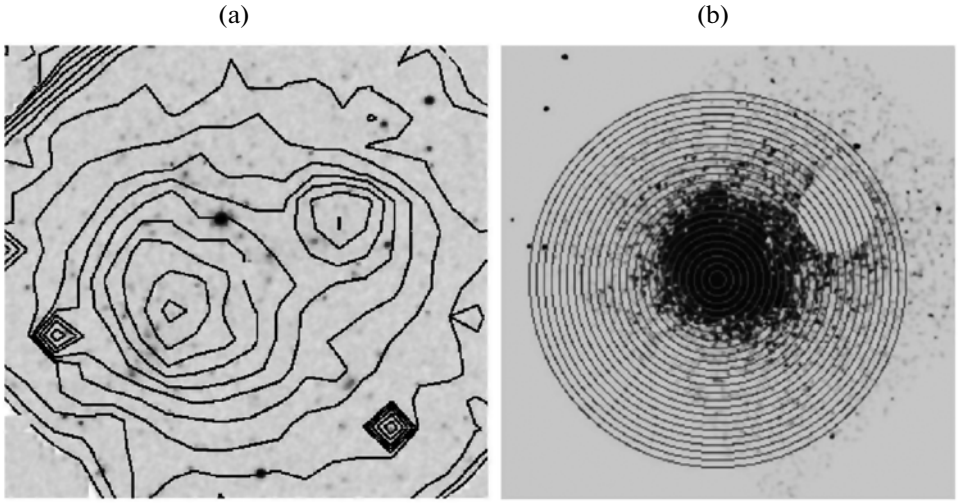

Fig. 1. The image of galaxy cluster A2744: the optic image with X-ray contours (DSS: archive.eso.org/dss/dss) (a), the image of A2744 in X-ray range after removing of the point sources and splitting on the rings (b).

ters of galaxies in [11]. Except the studies about a distribution of gas density, this model is widely used for the investigations of the other properties of gas in clusters: for example, in the work [6] β-model was used as an analog of NFW. Depending on the study aims, this model is often modified. In the works [24, 25] the two-dimensional β-model and KBB β-model (a generalized β-model which considers only an interior part of the object that allows to determine more accurately the maximum of the gas density profiles in the core) for the finding of the cluster surface brightness in X-ray images. It was shown that these modifications of the β-model are very successful.

The accurate estimates of the cluster total masses are very important for the cosmological models testing [2]. Such estimates can be done with a help of the X-ray observations of the hot intracluster gas in the galaxy clusters [27].

The aim of this work is to determine the content and the distribution of dark matter in galaxy cluster A2744 and also TO estimate the total mass of this cluster using the Chandra space observatory data. The other properties of the cluster as the luminosity the temperature, the density and the mass distribution of gas are also discussed in the paper.

For the calculations we used cosmological parameters: $H_0 = 73$ km s^{-1} Mpc^{-1}, $\Omega_m = 0.27$ and $\Omega_\Lambda = 0.73$.

2. OBSERVATIONAL DATA

The observation of cluster A2744 was performed in September 2001 with ACIS-S instrument of X-ray Chandra Observatory (ObsID 2212). The time of exposure is 25.14 ks [5]. The center of cluster has the equatorial coordinates $\alpha = 00^h14^m19.529^s$ and $\delta = -30°23'30.24''$ and redshift $z = 0.308$. A2744 consist of about 300 galaxies and has the visible diameter ~9′ according to NED [nedwww.ipac.caltech.edu].

The optical image of the cluster with X-ray contours is shown in Fig. 1a. It is known from the previous studies [15], that X-ray can be traced to a radius of 11' (3.7 Mpc). In works [15, 14], according to the observations of the space observatories Chandra and XMM-Newton, were shown that the maximum of X-ray radiation is located in the point with coordinates $\delta_{2000} = 00^h14^m18.7^s$, $\delta_{2000} = -30°23'16''$. The X-ray emission in A2744 is characterized by big number of sub-structures. In particular, one of them is situated at the distance of 150″ from the center of the cluster in the north-western side [14]. According to [1], the cooling time of A2744 (0.3×10^{11} years) is significantly larger than Hubble time that means that A2744 does not have any cooling flows.

For the preliminary data reduction we used the software CIAO version 4.2 [13]. First of all we found and removed all point sources (galaxies). We also did not consider the less massive component of the cluster with which, probably, the bigger component is in the interaction. The radius of the removed region is 0.8′.

After that we splitted the image on the concentric annuli with the same width (~40 kpc) (Fig. 1b). The outer radius of the largest ring is ~ 900 kpc.

The parameters of MEKAL model for each ring of the galaxy cluster A2744

N	kT, keV	norm (10^{-4} cm^{-5})	$\mathrm{Flux}_{0.3-7.0\,\mathrm{keV}}$ (10^{-13} erg/m^2)	χ^2
1	$9.86^{+2.51}_{-1.69}$	$3.16^{+0.1}_{-0.1}$	3.09	1.084
2	$14.74^{+3.93}_{-2.95}$	$4.26^{+0.16}_{-0.15}$	4.29	0.959
3	$10.47^{+1.91}_{-1.52}$	$5.05^{+0.13}_{-0.13}$	5.02	1.065
4	$8.39^{+1.11}_{-1.02}$	$5.56^{+0.13}_{-0.13}$	5.28	1.019
5	$10.16^{+1.76}_{-1.44}$	$5.90^{+0.15}_{-0.15}$	5.79	0.9099
6	$10.40^{+1.82}_{-1.53}$	$5.58^{+0.14}_{-0.14}$	5.49	1.041
7	$11.54^{+2.87}_{-2.01}$	$5.28^{+0.17}_{-0.15}$	5.25	0.6464
8	$10.68^{+2.49}_{-1.87}$	$4.67^{+0.14}_{-0.14}$	4.60	1.023
9	$9.36^{+1.94}_{-1.35}$	$4.35^{+0.12}_{-0.12}$	4.23	0.852
10	$8.40^{+1.67}_{-1.30}$	$4.09^{+0.11}_{-0.11}$	3.90	0.895
11	$10.42^{+2.94}_{-2.06}$	$3.56^{+0.13}_{-0.12}$	3.50	1.076
12	$8.82^{+2.46}_{-1.64}$	$2.99^{+0.1}_{-0.1}$	2.88	1.276
13	$9.04^{+2.94}_{-1.91}$	$2.65^{+0.1}_{-0.1}$	2.50	1.399
14	$8.53^{+3.04}_{-2.06}$	$2.26^{+0.09}_{-0.09}$	2.16	1.007
15	$8.14^{+3.15}_{-1.89}$	$2.02^{+0.09}_{-0.09}$	1.95	1.186
16	$9.28^{+4.11}_{-2.35}$	$1.90^{+0.09}_{-0.08}$	1.84	1.2
17	$9.37^{+6.85}_{-2.81}$	$1.66^{+0.1}_{-0.08}$	1.61	1.616
18	$8.65^{+3.83}_{-2.19}$	$1.62^{+0.08}_{-0.08}$	1.58	1.787
19	$7.52^{+6.64}_{-2.38}$	$1.34^{+0.09}_{-0.08}$	1.25	1.343
20	$6.08^{+2.61}_{-1.53}$	$1.19^{+0.08}_{-0.08}$	1.09	1.703

For each ring separately we built the spectrum which was fitted by the WABS*MEKAL model in the Xspec software version 12.6 [3], here the WABS parameter was used for describing of the galactic absorption (for the A2744 $n_H = 1.6 \times 10^{20}$ cm^{-2} [7]); MEKAL is the model developed by [17] which describes an emission that comes from a hot diffuse plasma. For each ring we determined the temperature kT and parameter $norm \sim \int n_e n_H dV$ which is proportional to the electron and hydrogen concentrations for 0.4–7.0 keV energy range. Note, that the other parameters of model were fixed. The content of heavy elements was taken near the solar level ($Z = 0.3$). We also determined the value of flux for the energy range 0.4–7.0 keV. The parameters kT and $norm$ can be seen in table, N corresponds to the number of ring counting from the center.

The spectrum of one of the rings, which was fitted by MEKAL model, is shown in Fig. 2. The temperature profile (from center to the cluster periphery) is shown in Fig. 3. For further modelling we selected the average value of the temperature $\langle T \rangle = 9.82^{+0.41}_{-0.43}$ keV that corresponds to the horizontal line in Fig. 3. Note, that this value of the temperature corresponds to the redshift of this cluster $z = 0.308$.

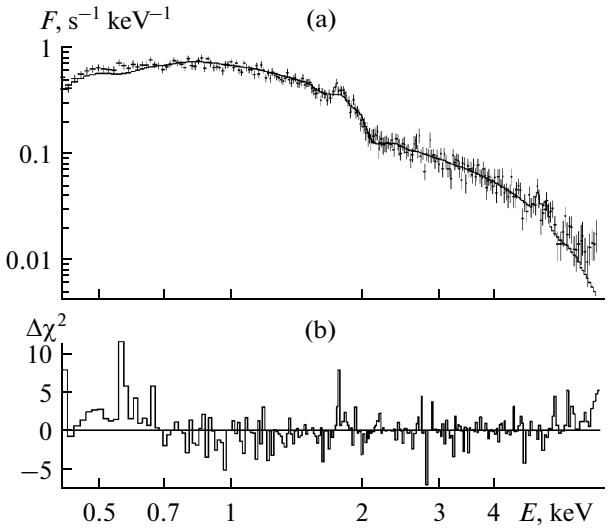

Fig. 2. The spectrum of cluster for one ring fitted by WABS*MEKAL model.

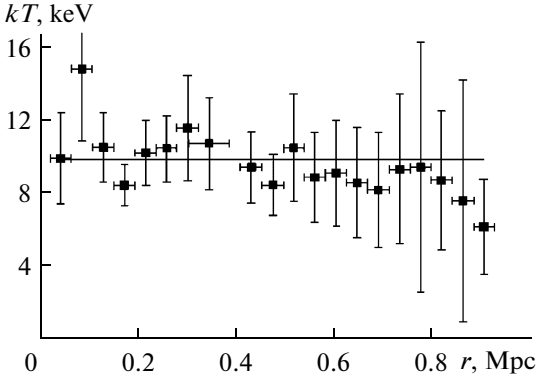

Fig. 3. The temperature profile of galaxy cluster A2744.

This value of the average temperature within errors is in a good agreement with work [14] (10.1 keV) and works [12, 15] ($9.3^{+4.9}_{-2.7}$ keV).

3. THE SURFACE BRIGHTNESS PROFILE MODELLING

We have made the numerical simulations for the reconstruction of the distribution of hot gas and dark matter in the galaxy cluster A2744. For the density profile of dark matter we used the NFW model:

$$\rho(r) = \frac{\rho_0}{\left(\frac{r}{r_s}\right)\left(1+\frac{r}{r_s}\right)^2}, \quad (1)$$

where ρ_0 is the characteristic density of dark matter and r_s is the characteristic radius of dark matter halo, and r is the radius for which the density is calculated. If we know the density of dark matter then we can find the total mass of dark matter within given radius:

$$M(<r) = 4\pi\int_0^r \rho(r')r'^2 dr' = 4\pi\rho_0 r_s^3\left[\ln\left(1+\frac{r}{r_s}\right) - \frac{r}{r_s+r}\right]. \quad (2)$$

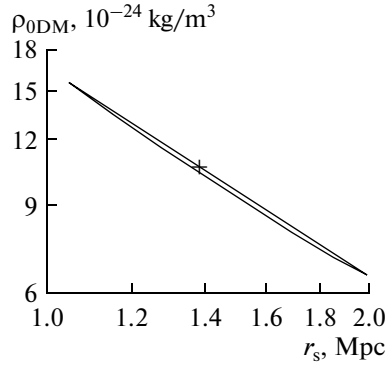

Fig. 4. The area of values of the dark matter density ρ_0 and the radius r_s with 90% confidence level for galaxy cluster A2744.

A massive halo of dark matter creates the gravitational field in which the distribution of hot gas is formed. The gravitational potential ϕ of dark matter can be found by formula

$$\frac{d\phi}{dr} = G\frac{M(<r)}{r^2}. \tag{3}$$

All the following computations we made taking into account the hydrostatic equilibrium condition of the X-ray emitting gas in galaxy cluster and assumption that the $T_g = \text{const}$. We can write the hydrostatic equilibrium condition as follows:

$$\nabla P = -\rho_g \nabla\phi(r), \tag{4}$$

where P and g are the gas pressure and the density respectively. Since the density and pressure of hot gas have very low values, we can use the ideal gas law as follows $P = \rho_g kT_g/\mu m_p$. In the result we obtained the equation for unknown gas density distribution

$$\frac{\nabla\rho_g}{\rho_g} = -\nabla\phi(r)\frac{\mu m_p}{kT_g}. \tag{5}$$

For the construction of the hot gas density field we had to calculate numerically the system of the differential equations:

$$\frac{1}{\rho_g}\frac{\partial\rho_g}{\partial x_i} = -\frac{\mu m_p}{kT_g}\frac{\partial\phi(r)}{\partial x_i}, \tag{6}$$

where $x_i = (x, y, z)$ are the Cartesian coordinates.

After the radial construction of the gas density ρ_g in the cluster we found the surface brightness profile in X-ray range. The emission flux, that comes from the observed regions, is proportional to the integral density of hot gas in a square ρ_g^2 along the line of sight. According to work [27], for the plasma in the cluster, we took $n_e/n_p = 1.17$ and $\rho_g = 1.35 m_p n_p$, where n_e and n_p are the electron and proton concentrations, respectively. We have to note that from modelling we can obtain the gas density with precision of some constant factor a which depends on the boundary conditions in the integration (6). Therefore the real density ρ_g^{real} of gas is equal to $\rho_g^{\text{real}} = a\rho_g^{\text{sim}}$, where ρ_g^{sim} is the density of gas obtained from the simulations. So, we can write $\rho_g^{\text{sim}} \equiv \rho_g$ in (6). Thus the value of emission EM_{sim} can be found from the modelling:

$$EM_{\text{sim}} = \int n_e n_p dV = 0.64/m_p^2 \int (\rho_g^{\text{sim}})^2 dV. \tag{7}$$

Using the equation (7) we can found

$$\text{norm}_{\text{sim}} = EM_{\text{sim}} \times 10^{-14}/[4\pi(D_A(1+z))^2], \tag{8}$$

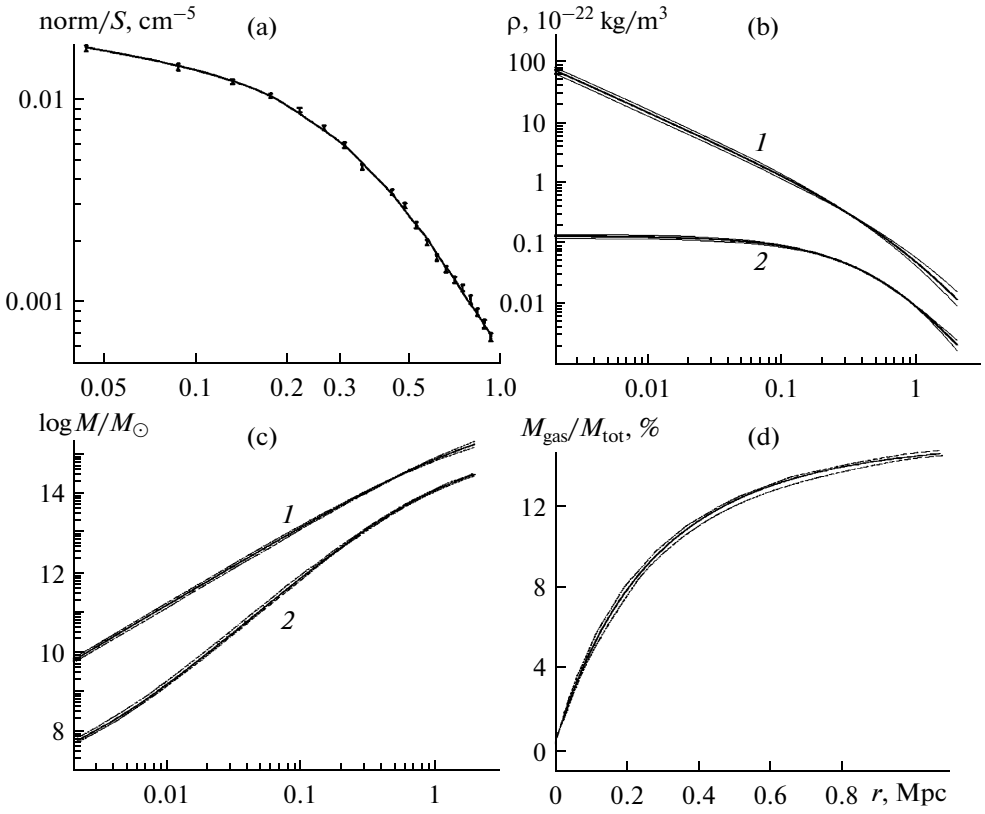

Fig. 5. Obtained distributions of some parameters of galaxy cluster A2744: the surface brightness profile (points correspond to the observational data, line corresponds to the model fitting) (a), the density and mass profiles for dark matter (*1*) and hot intracluster gas (*2*) (b), (c), the fraction of mass of the gas in the total mass of the cluster (d).

where D_A is the angular distance to the A2744. From the observations we obtained the parameter $\mathrm{norm}_{\mathrm{MEKAL}}$ which was fitted by the $\mathrm{norm}_{\mathrm{sim}}$ from the simulations. Since the $\mathrm{norm}_{\mathrm{MEKAL}}$ parameter can be found as

$$\mathrm{norm}_{\mathrm{MEKAL}} = \frac{0.64}{m_p^2}\int\frac{(\rho_g^{\mathrm{real}})^2 dV\times 10^{-14}}{[4\pi(D_A(1+z))^2]}, \tag{9}$$

then using the equations (7, 8) and (9) we can found the constant factor a

$$a = \sqrt{\frac{\mathrm{norm}_{\mathrm{MEKAL}}}{\mathrm{norm}_{\mathrm{sim}}}}. \tag{10}$$

So, we got the hot gas density $\rho_g^{\mathrm{real}} = a\rho_g^{\mathrm{sim}}$ and estimated the value of emission EM_{real} replacing ρ_g^{sim} in equation (7) by ρ_g^{real}.

4. RESULTS

In our model we used two free parameters ρ_0 and r_s. Sorting them out in the acceptable ranges we selected such pair of values which is the best convenient for describing the observational cluster profile. Using the χ^2 test we found the area of values ρ_0 and r_s with 90% confidence level: $r_s = 1.38^{+0.56}_{-0.34}$ Mpc, $\rho_0 = 1.05^{+0.50}_{-0.38} \times 10^{-23}$ kg/m^3; $\chi^2 = 1.1$ (cross on the Fig. 4). These parameters are in a good agreement with the values from [14] ($r_s = 1.1^{+0.3}_{-0.4}$ Mpc and $\rho_0 = 1.2^{+0.4}_{-0.6} \times 10^{-23}$ kg/m^3) and were used for the fitting of the surface brightness profile of considered cluster.

The observed surface profile (points) and its approximation by our model (solid line) are shown in Fig. 5. In Fig. 5 the density profiles of dark matter (1) and hot gas (2) are shown. We estimated the value of radius R_{200} and the total mass M_{200} within this radius. Radius R_{200} is a distance from the center of cluster where the density is equal to the value of the critical density ρ_c that is increased in 200 times. Since the value of critical density is $\rho_c = 1.335 \times 10^{-26}$ kg/m^3 for $z = 0.308$ ($\rho_{cr}(z) = 3E(z)^2 H_0^2/8\pi G$, where $E^2(z) = \Omega_m(1+z)^3 + \Omega_\Lambda$), then $200\rho_c$ corresponds to the radius $2.38^{+0.36}_{-0.31}$ Mpc. For this radius we found the total mass of the cluster $M_{200} = 2.22^{+0.13}_{-0.12} \times 10^{15} M_\odot$. The values of dark matter and gas within R_{200} are $1.88^{+0.18}_{-0.21} \times 10^{15} M_\odot$ and $3.31^{+0.17}_{-0.25} \times 10^{14} M_\odot$, respectively. The mass distributions of dark matter (1) and gas (2) are shown in Fig. 5.

The fraction of gas in the total mass of cluster is shown (in the %) in Fig. 5.

It can be seen that the fraction of gas in the total mass of A2744 within the R_{200} is $15.4^{+1.3}_{-1.3}$ % and the dark matter content is $84.6^{+1.4}_{-1.3}$ %. These values are in a good agreement with data [1] in the same radius ranges: $M_{\rm gas}/M_{\rm total} = 0.15^{+0.12}_{-0.11}$. Meanwhile the authors [14] obtained 8–12%.

5. CONCLUSIONS

In the result of the X-ray data reduction by Chandra we obtained the following values of parameters for galaxy cluster Abell 2744.

1. The average temperature of the cluster is $\langle T \rangle = 9.82^{+0.41}_{-0.43}$ keV.

2. The values of the characteristic parameters of the cluster (the density of dark matter and the characteristic radius): $\rho_0 = (1.05^{+0.50}_{-0.38}) \times 10^{-23}$ kg/m^3 and $r_s = (1.38^{+0.56}_{-0.34})$ Mpc.

3. The values of density of the dark matter, intracluster gas and total mass M_{200} within R_{200} ($2.38^{+0.36}_{-0.31}$) Mpc from the center of the cluster): $\rho_{DM} = 8.19^{+1.65}_{-1.69} \times 10^{-25}$ kg/m^3, $\rho_g = 1.44^{+0.39}_{-0.25} \times 10^{-25}$ kg/m^3 and $M_{200} = 2.22^{+0.13}_{-0.12} \times 10^{15} M_\odot$, respectively.

4. The fraction of gas and dark matter in the total mass of cluster: $15.4^{+1.3}_{-1.3}$ % and $84.6^{+1.4}_{-1.3}$ %, respectively.

This study was done using the archival data by Chandra and with a help of the Chandra X-ray Center software (CIAO 4.2). The authors would like to thank the project team by creating of the high-quality Chandra X-ray observations archive. We thank the referee for the careful checking of the paper and useful comments.

The work is partially supported by "Kosmomikrofizyka" program of NAS of Ukraine.

REFERENCES

1. S. W. Allen and A. C. Fabian, "The Relationship between Cooling Flows and Metallicity Measurements for X-Ray-Luminous Clusters," Mon. Not. R. Astron. Soc. **297**, 63–68 (1998).
2. S. W. Allen, R. W. Schmidt, and A. C. Fabian, "The X-Ray Virial Relations for Relaxed Lensing Clusters Observed with Chandra," Mon. Not. R. Astron. Soc. **328**, 37–41 (2001).
3. K. Arnaud, "Astronomical Data Analysis Software and Systems," ASP Conf. **101**, 17 (1996).
4. H. Boehringer and W. Norbert, "X-Ray Spectroscopy of Galaxy Clusters," Astron. Astrophys. Rev. **18**, 127–196 (2010).
5. W. Boschin, "A Deep Cluster Survey in Chandra Archival Data. First Results," Astron. Astrophys. **396**, 397–409 (2002).
6. A. Cavaliere and R. Fusco-Femiano, "X-Rays from Hot Plasma in Clusters of Galaxies," Astron. Astrophys. **49**, 137–144 (1976).
7. J. M. Dickey and F. J. Lockman, "H I in the Galaxy," Ann. Rev. Astron. Astrophys. **28**, 215–261 (1990).
8. R. Demarco, F. Magnard, F. Durret, and I. Marquez, "A Study of Dark Matter Halos and Gas Properties in Clusters of Galaxies from ROSAT Data," Astron. Astrophys. **407**, 437–451 (2003).
9. H. Ebeling, W. Voges, H. Bohringer, et al., "Properties of the X-Ray-Brightest Abeel-Type Clusters of Galaxies (XBACs) from ROSAT All-Sky Survey Data. I," Mon. Not. R. Astron. Soc. **281**, 799–829 (1996).

10. A. E. Evrard, C. A. Metzler, and J. F. Navarro, "Mass Estivates of X-Ray Clusters," Astrophys. J. **469**, 494–507 (1996).
11. A. Ginoguenov, T. H. Reiprich, and H. Bohringer, "Details of the Mass-Temperature Relation for Clusters of Galaxies," Astron. Astrophys. **368**, 749–759 (2001).
12. T. F. Frederiksen, S. H. Hansen, O. Host, et al., "Determining All Gas Properties in Galaxy Clusters from the Dark Matter Distribution Alone," Astrophys. J. **700**, 1603–1608 (2009).
13. A. Fruscione, J. C. McDowell, G. E. Allen, et al., "CIAO: Chandra's Data Analysis System," in *Observatory Operations: Strategies, Processes and Systems,* Ed. by D. Silva and R. Doxsey, Proc. SPIE **6270**, 6271V (2006).
14. F. Govoni, L. Feretti, H. Bohringer, et al., "Radio and X-Ray Diffuse Emission in Six Clusters of Galaxies," Astron. Astrophys. **376**, 803–819 (2001).
15. J. C. Keimpne and L. P. David, "A Chandra View of the Multiple Merger in Abell 2744," Mon. Not. R. Astron. Soc. **349**, 385–392 (2004).
16. N. Makino and K. Asano, "Cluster Mass Estimate and a Cusp of the Mass-Density Dirtibution in the Clusters of Galaxies," Astrophys. J. **512**, 9–20 (1999).
17. R. Mewe, J. S. Kaastra, and D. A. Liedahl, "Update of MEKA: MEKAL," Legacy **6**, 16 (1995).
18. B. Moore, T. Quinn, F. Governato, et al., "Cold Collapse and the Core Catastrophe," Mon. Not. R. Astron. Soc. **310**, 1147–1152 (1999).
19. J. F. Navarro, C. S. Fhenk, and S. D. White, "Simulations of X-Ray Clusters," Mon. Not. R. Astron. Soc. **275**, 720–740 (1995).
20. J. F. Navaroo, C. S. Frenk, and S. D. White, "The Structure of Cold Dark Matter Halos," Astrophys. J. **462**, 563–575 (1996).
21. E. Pointecouteau, M. Arnaud, J. Kaastra, et al., "XMM-Newton Observation of the Relaxed Cluster A478: Gas and Dark Matter Distribution from $0.01R_{200}$ to $0.5R_{200}$," Astron. Astrophys. **423**, 33–47 (2004).
22. E. Pointecouteau, M. Arnaud, and G. W. Pratt, "Probing the Dark Matter Profile of Hot Clusters and the M-T Relations with XMM-Newton," Adv. Space Res. **36**, 659–662 (2005).
23. E. Pointecouteau, M. Arnaud, and G. W. Pratt, "The Structural and Scaling Properties of Nearby Galaxy Clusters. I. The Universal Mass Profile," Astron. Astrophys. **435**, 1–7 (2005).
24. G. W. Pratt and M. Arnaud, "The Mass Profile of A1413 Observed with XMM-Newton: Implications for the M-T Relation," Astron. Astrophys. **394**, 375–393 (2002).
25. G. W. Pratt and M. Arnaud, "XMM-Newton Observation A1413," in *Matter and Energy Clusters of Galaxies*, ASP Conf. Proc. **301**, 555 (2003).
26. R. Sadat, "Cluster of Galaxies and Mass Estimates," in *From Quantum Fluctuations to Cosmological Structures, Proceedings of the International School in Astrophysics* (Casablanca, Morocco, 1997), p. 18.
27. A. Vikhlinin, W. Forman, and C. Jones, "Outer Regions of the Cluster Gaseous Atmospheres," Astrophys. J. **525**, 47–57 (1999).
28. X. Wu and Y. Xue, "On the Radial Density Profile of Intracluster Gas Tracing the Isothermal Dark Halo with a Finite Core," Astrophys. J. **542**, 578–587 (2000).
29. F. Zwicky, "On the Masses of Nebulae and of Clusters of Nebulae," Astrophys. J. **86**, 217–246 (1937).